FEMS Microbiology Ecology, 2024, **100**, 1–14
DOI: 10.1093/femsec/fiae001
Advance access publication date: 10 January 2024
Research Article

Seafloor incubation experiments at deep-sea hydrothermal vents reveal distinct biogeographic signatures of autotrophic communities

Heather Fullerton [1,*], Lindsey Smith[2], Alejandra Enriquez[1], David Butterfield[3], C. Geoffrey Wheat[4], Craig L. Moyer[2]

[1]Department of Biology, College of Charleston, 66 George Street, Charleston, SC 29424, United States
[2]Department of Biology, Western Washington University, 516 High St, Bellingham, WA 98225, United States
[3]Cooperative Institute for Climate, Ocean, and Ecosystem Studies, University of Washington and NOAA/PMEL, John M. Wallace Hall, 3737 Brooklyn Ave NE, Seattle, WA 98105, United States
[4]Institute of Marine Studies, College of Fisheries and Ocean Sciences, University of Alaska Fairbanks, 2150 Koyukuk Drive, 245 O'Neill Building, PO Box 757220, Fairbanks, Alaska 99775-7220, United States
*Corresponding author. Department of Biology, College of Charleston, 66 George Street, Charleston, SC 29424, United States. E-mail: fullertonhe@cofc.edu
Editor: [Lee Kerkhof]

Abstract

The discharge of hydrothermal vents on the seafloor provides energy sources for dynamic and productive ecosystems, which are supported by chemosynthetic microbial populations. These populations use the energy gained by oxidizing the reduced chemicals contained within the vent fluids to fix carbon and support multiple trophic levels. Hydrothermal discharge is ephemeral and chemical composition of such fluids varies over space and time, which can result in geographically distinct microbial communities. To investigate the foundational members of the community, microbial growth chambers were placed within the hydrothermal discharge at Axial Seamount (Juan de Fuca Ridge), Magic Mountain Seamount (Explorer Ridge), and Kama'ehuakanaloa Seamount (Hawai'i hotspot). Campylobacteria were identified within the nascent communities, but different amplicon sequence variants were present at Axial and Kama'ehuakanaloa Seamounts, indicating that geography in addition to the composition of the vent effluent influences microbial community development. Across these vent locations, dissolved iron concentration was the strongest driver of community structure. These results provide insights into nascent microbial community structure and shed light on the development of diverse lithotrophic communities at hydrothermal vents.

Keywords: Axial Seamount; Campylobacterota; community structure; hydrothermal vents; Kama'ehuakanaloa Seamount; Magic Mountain Seamount; Zetaproteobacteria

Introduction

Deep-sea hydrothermal vents are dynamic and extremely productive biological ecosystems supported by chemosynthetic microbial populations (Jannasch and Mottl 1985). These ecosystems offer multiple unique circumstances for microbial growth, including substrate surrounding and near vent discharge, within the subsurface, plume emissions, and through the formation of symbiotic relationships with vent invertebrates (Karl et al. 1980, Jannasch 1983, Murdock et al. 2021). The hydrothermal vents themselves provide energy to the microorganisms via the oxidation of reduced solutes that discharge from these habitats (Dick 2019). Overall, the metabolic capacity of the system depends on the chemical composition of the hydrothermal vent effluent (Karl 1995, Nakagawa and Takai 2008). The concentrations of reduced solutes can vary over space and time, and rapid changes in vent chemistry and temperature impact microbial community composition, structure, and function (Butterfield et al. 1997, Danovaro et al. 2017). Microbial species are often found at hydrothermal vents that are geographically separated; therefore, they are ideal systems for addressing questions of microbial biogeography and speciation (Price et al. 2015, Duchinski et al. 2019). In these habitats, there is evidence of dispersal as well as allopatric speciation in both bacteria and archaea (Price et al. 2015, Mino et al. 2017).

Bacteria within the Campylobacterota and Proteobacteria phyla are often found near hydrothermal vents. Campylobacteria and Zetaproteobacteria are two of the major phylogenetic classes of Bacteria distributed below the subsurface, within the vent effluent, and near the vent orifice. Such bacteria form microbial biofilms, also referred to as microbial mats (Waite et al. 2017, 2018, Parks et al. 2018). Many of the dominant organisms at hydrogen- and sulfur-rich hydrothermal vents are grouped within the phylum Campylobacterota and class Campylobacteria (formerly Epsilonproteobacteria) with *Sulfurimonas*, *Sulfurovum*, *Nitratiruptor*, *Thioreductor*, and *Arcobacter* as the most common genera (Orcutt et al. 2011b). In contrast, at hydrothermal vent systems with high concentrations of reduced iron, the class Zetaproteobacteria is the dominant community member (Hager et al. 2017, Duchinski et al. 2019). They are the newest described class of Proteobacteria with one described genus, *Mariprofundus* (Emerson et al. 2007, Makita et al. 2017). Since their original identification at hydrothermal vents, Zetaproteobacteria have been shown to reside in specific ecological niches dispersed worldwide (McAllister et al. 2019).

Received 23 May 2023; **revised** 20 October 2023; **accepted** 9 January 2024

Campylobacterota are found in diverse environments, have diverse metabolic strategies (Campbell et al. 2006), and in many hydrothermal vent ecosystems, members of the phylum Campylobacterota have been classified as the primary producers (Han and Perner 2015). Within this phylum, *Sulfurimonas* and *Sulfurovum* have been identified in active and inactive hydrothermal sulfides at the East Pacific Rise (Sylvan et al. 2012a), microbial mats of the Mariana Arc and back-arc (Hager et al. 2017), vent effluent of the Mariana Arc and Axial Seamount (Huber et al. 2010, Akerman et al. 2013), and hydrothermal sediments of the Mid-Atlantic Ridge (Cerqueira et al. 2018). *Sulfurimonas* spp. are able to grow with reduced sulfur compounds and hydrogen as their electron donor and aerobically with oxygen or anaerobically with nitrate or nitrite as their electron acceptors (Vetriani et al. 2014, Han and Perner 2015). *Sulfurimonas autotrophica* was isolated from the Mid-Okinawa Trough hydrothermal field and grows autotrophically with sulfide, elemental sulfur, and thiosulfate as electron donors (Inagaki et al. 2003). Genomic analysis of the globally distributed *Sulfurimonas* shows evidence of allopatric speciation and suggests that geographic distance is the primary driver of genetic variation (Mino et al. 2017).

At iron-dominated venting locations, Zetaproteobacteria are considered microbial ecosystem engineers (Hager et al. 2017). This means they have the potential to modulate the flow of organic carbon to other microbes and can shape their habitat by producing iron oxyhydroxide minerals and exopolysaccharides, increasing richness and diversity within the microbial landscape, affecting the health and stability of the environment (Chan et al. 2011, 2016a, Jesser et al. 2015, Hager et al. 2017). Even at low abundances, Zetaproteobacteria can impact their local environment and can also be considered keystone taxa, because they are necessary for the survival of other microbes and are drivers of ecosystem biodiversity (Beam et al. 2018). There are currently 59 OTUs of Zetaproteobacteria (zOTUs), four of which are considered cosmopolitan and another 12–15 of which have high endemic abundances. The remaining zOTUs have rarely been observed (McAllister et al. 2019). A few isolates have been grown in pure culture including *Mariprofundus ferrooxydans* (strains PV-1 and JV-1) from Kama'ehuakanaloa Seamount and isolates from the estuarine water column of Chesapeake Bay, among others (Chiu et al. 2017). However, the cosmopolitan zOTUs, which are ubiquitous at iron-driven vent communities throughout the Pacific and Atlantic Oceans, have not yet been cultured (McAllister et al. 2011, Scott et al. 2015). Therefore, the physiology of these cosmopolitan zOTUs has been inferred from the distantly related isolates and metagenomics (Field et al. 2015, Fullerton et al. 2017, He et al. 2017).

With the exception of an earlier pilot-study using T-RFLP analysis that focused on the development of microbial mats (Engebretson 2002), microbiological studies at Axial and Magic Mountain have been conducted on fluid samples to assess microbial vent-associated community structure (Huber et al. 2003, Meyer et al. 2013a, Anderson et al. 2017, Fortunato et al. 2018, Moulana et al. 2020). A previous study using microbial growth chambers (MGC) at Kama'ehuakanaloa Seamount (formerly known as Lō'ihi Seamount) identified Zetaproteobacteria as the dominant colonizers (Rassa et al. 2009). MGCs provide an inert surface to examine nascent communities of lithotrophs to better understand how microbial communities rebuild and interact. To further investigate how microbial communities develop across geographically diverse hydrothermal vents, MGCs were deployed within the hydrothermal discharge at Axial Seamount (Juan de Fuca Ridge), Magic Mountain Seamount (Explorer Ridge), and Kama'ehuakanaloa Seamount (Hawai'i hotspot). The analysis of the nascent communities and comparisons across distinct hydrothermal vents addresses how microbial communities develop and how diversity is established within these complex ecosystems.

Materials and methods

Construction of MGCs

MGCs were constructed with three 3″ sections of plexiglass cylinders that were enclosed on top and bottom with 202 μm Nytex mesh to restrict grazing by macrofauna (Rassa et al. 2009). Each of the three chambers contained a total of ∼300 g of hand-woven 8 μm silica wool (yielding ∼33 m^2 of surface area) as a fresh surface to facilitate microbial attachment and growth. Negative buoyancy was achieved by the addition of a stainless-steel eyebolt in the center of the three chambers, which also served as an attachment point for a polyurethane line for ease of deployment and collection.

Sample collection

The MGCs were incubated from 2 to 19 days at venting locations at three different hydrothermal vent sites (1) Axial Seamount, (2) Magic Mountain, and (3) Kama'ehuakanaloa Seamounts. Vent locations, deployment and *in situ* incubation times are summarized in Table 1. MGC names consist of location and chamber number, with Ax denoting Axial Seamount, Ex for Magic Mountain, and L for Kama'ehuakanaloa. At Kama'ehuakanaloa, MGCs were deployed using the submersible *PISCES V* and the remotely operated vehicle (ROV) *JASON* in 1998, 2004, and 2009. At Magic Mountain, MGCs were deployed and collected with the ROV *ROPOS* in 2002. At Axial, MGCs were deployed using the ROV *ROPOS* in 1998, 1999, 2000, and 2002. In all cases, temperatures were monitored by either HOBO miniature temperature recorders placed at the same location as the MGC or by a temperature probe attached to the manipulator of the ROV at the time of MGC deployment and recovery. Upon recovery, each MGC was placed in a sealed box at the seafloor to minimize disturbance and flushing of the chambers during assent and recovery of the vehicle. Immediately upon recovery, MGCs were aseptically penetrated and silica wool removed, placed into heavyweight Ziploc-style sample bags, and immediately frozen. The frozen samples were shipped and stored at −80°C until further processing in the laboratory.

For the Axial and Magic Mountain locations, hydrothermal discharge was collected with the hydrothermal fluid and particle sampler. An aliquot was analyzed on board for total hydrogen sulfide and pH using standard colorimetric and electrode techniques (Butterfield et al. 2004). An aliquot was acidified and analyzed ashore for dissolved iron and manganese by atomic absorption. Similarly, hydrothermal fluids that discharged from the Kama'ehuakanaloa Seamount were collected using Walden-Weiss titanium syringe ("Major") samplers (Von Damm et al. 1985). Aliquots were measured at sea for total hydrogen sulfide and pH using the same methods as described previously (Butterfield et al. 2004). Dissolved Mn and Fe were measured ashore using standard inductively coupled plasma optical emission spectrometry technique (Wheat et al. 2017).

Isolation of microbial biomass

Silica wool was thawed on ice and then washed with sterile 1X PBS at 4°C for 30 min in sterile mason jars on a rotating platform. This wash solution was then decanted into 50 ml conical tubes for centrifugation at 6000 × *g* for 15 min at 4°C. The supernatant

Table 1. *In situ* incubation times, location, cruise year, marker, and temperature of incubation for each MGC.

MGC	Duration (days)	Location	Cruise Year	Marker	Temperature (°C)	Observed	Simpson
AxMGC-01	2	Axial Caldera	1998	N4	23.1	117	0.66
AxMGC-03	4	Axial Caldera	1998	113	22.3	1278	0.95
AxMGC-05	16	Axial Caldera	1998	33	28.2	102	0.91
AxMGC-08	2	Axial Caldera	1998	33	28.2	840	0.81
AxMGC-10	14	Axial Caldera	1998	33	28.2	186	0.95
AxMGC-18	12	Axial Caldera	1998	N2	8.0	861	0.86
AxMGC-36	5	Axial Caldera	1999	N4	17.0	983	0.71
AxMGC-38	5	Axial Caldera	1999	N4	17.0	626	0.68
AxMGC-43	5	Axial Caldera	1999	33	63.8	449	0.91
AxMGC-44	7	Axial Caldera	2000	33	26.0	617	0.95
AxMGC-47	7	Axial Caldera	2000	N4	15.0	843	0.96
AxMGC-66	19	Axial Caldera	2002	N6	8.5	1144	0.97
ExMGC-03	4	Magic Mountain	2002	73	21.0	544	0.94
ExMGC-04	4	Magic Mountain	2002	81	11.5	140	0.95
LMGC-L7	4	Kama‘ehuakanaloa	1998	20	24.0	796	0.94
LMGC-L9A	4	Kama‘ehuakanaloa	1998	11	77.0	207	0.90
LMGC-L10	4	Kama‘ehuakanaloa	1998	11	64.0	339	0.87
LMGC-03	4	Kama‘ehuakanaloa	2004	29	18.0	1791	0.94
LMGC-04	4	Kama‘ehuakanaloa	2004	30	60.0	1012	0.93
LMGC-05	4	Kama‘ehuakanaloa	2004	38	44.0	947	0.92
LMGC-07	4	Kama‘ehuakanaloa	2004	38	44.0	1534	0.93
LMGC-08	4	Kama‘ehuakanaloa	2004	39	46.0	1022	0.94
LMGC-09	4	Kama‘ehuakanaloa	2004	36	54.0	1728	0.95
LMGC-10	4	Kama‘ehuakanaloa	2004	36	54.0	996	0.89
LMGC-89	5	Kama‘ehuakanaloa	2009	39	47.5	202	0.84
LMGC-90	8	Kama‘ehuakanaloa	2009	57	12.5	1382	0.82
LMGC-91	5	Kama‘ehuakanaloa	2009	39	46.0	107	0.93
LMGC-92	9	Kama‘ehuakanaloa	2009	57	24.3	1074	0.77
LMGC-93	8	Kama‘ehuakanaloa	2009	36	35.6	242	0.95
LMGC-94	8	Kama‘ehuakanaloa	2009	57	25.1	931	0.82
LMGC-96	8	Kama‘ehuakanaloa	2009	38	50.2	129	0.94
LMGC-97	9	Kama‘ehuakanaloa	2009	57	25.1	756	0.84
LMGC-98	9	Kama‘ehuakanaloa	2009	34	50.6	281	0.96

was returned to the mason jar for another 1X PBS wash and the cell pellet was stored at 4°C. This process was completed until the 1X PBS was clear. Cell pellets were combined, and then aliquoted into ~0.5 g wet weight for DNA extraction.

DNA extractions, sequencing, and sequence processing

Genomic DNA was extracted from cell pellets using the Fast DNA SPIN Kit for Soil (MP Biomedicals, Santa Ana, CA) according to the manufacturer's protocol with a minor modification in which the gDNA was eluted in 1.0 mM Tris with 0.01 mM EDTA at pH 8. Cell lysis was optimized using two rounds of bead beating for 45 s at a power setting of 5.5 using the FastPrep instrument (MP Biomedicals) with samples being placed on ice between runs. Extracted DNA was quantified by a Qubit 2.0 fluorometer using high-sensitivity reagents (ThermoFisher Scientific, Waltham, MA).

The V3–V4 regions of the SSU rRNA gene were amplified via polymerase chain reaction from all MGC samples using bacterial primers 340F and 784R (Klindworth et al. 2013, Hager et al. 2017). The resulting amplicons were sequenced using a MiSeq (Illumina, San Diego, CA) as per the manufacturer's protocol generating 2 × 300 bp paired-end reads. The resulting reads were trimmed of primers using CutAdapt (Martin 2011). The trimmed reads were then processed using the Divisive Amplicon Denoising Algorithm 2 (DADA2) v1.26.0 with pseudopooling following the previously described protocols (Lee et al. 2015, Callahan et al. 2016, 2017) with R version 4.01 and using the Silva v138 database for assigning taxonomy. Samples were normalized using a center log-ratio transformation as implemented with microbiome version 1.10.0 in R (Lahti and Shetty 2017). Further analysis was completed using phyloseq version 1.32 (McMurdie and Holmes 2013). Differentially abundant ASVs were determined using DESeq2 (Love et al. 2014). Analysis of Zeta OTUs was completed on SILVA-aligned Zetaproteobacteria identified sequences with ZetaHunter (McAllister et al. 2018). The network was developed using the top 0.5% amplicon sequence variants (ASVs) by mean relative abundance, a total of 41 ASVs. Network construction and analysis were performed using the NetCoMi package for R (Peschel et al. 2021), employing the "propr" measure for estimating associations (Lovell et al. 2015, Erb and Notredame 2016, Erb et al. 2017, Quinn et al. 2017, 2018, 2019) and the "SPRING" method for visualizing associations (Yoon et al. 2019) and an eigenvector centrality cutoff of 0.95.

Results

Site descriptions

MGCs at the time of placement and recovery of representative short-term incubations are shown in Fig. 1. At Kama‘ehuakanaloa,

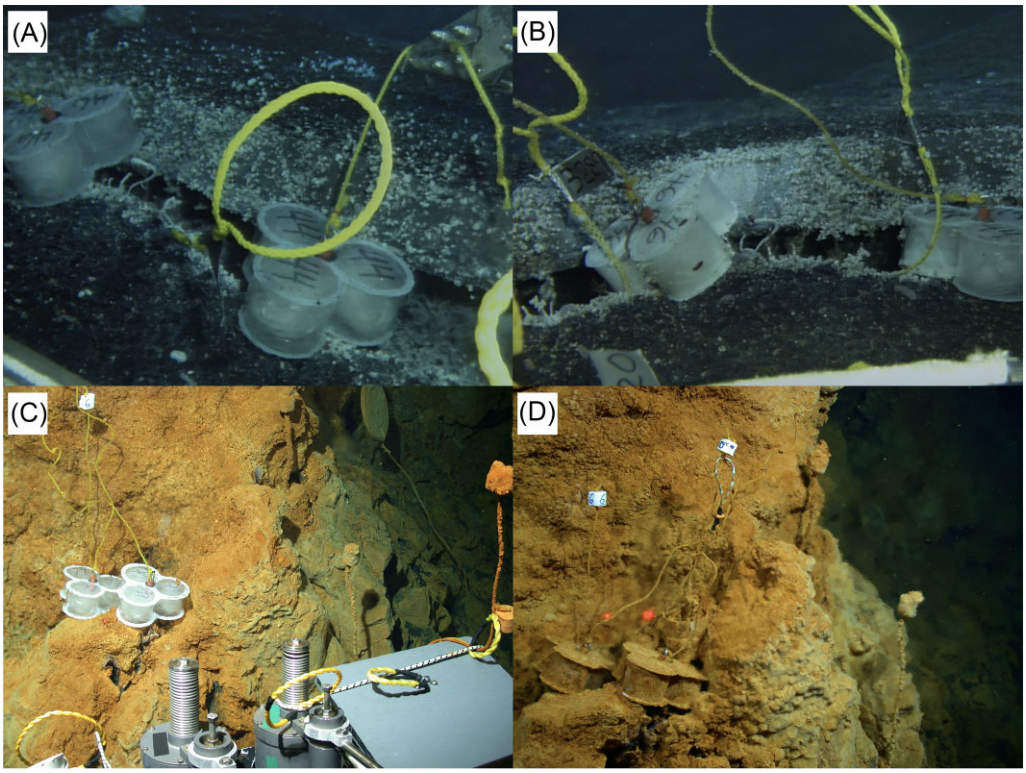

Figure 1. Pictures of representative MGCs before and after incubation show microbial biomass development as indicated in changes in opacity and color. (A) AxMGC.44 and AxMGC.46 at the time of placement. (B) AxMGC.44 and AxMGC.46 at recovery after 7 days. (C) LMGC.77 and LMGC.79 at the time of placement. (D) LMGC.77 and LMGC.79 at the time of recovery after 13 days.

Hiolo North is represented by Markers 31, 36, and 39, Hiolo South is represented by Markers 34 and 38, and Pohaku is represented by Marker 57 (Figure S1, Supporting Information). MGCs from Explorer Ridge were incubated at two vent sites at the Magic Mountain field on Explorer Ridge (Figure S2, Supporting Information). MGCs were incubated at four vent sites in the SE caldera of Axial Seamount, over a distance of 3 km from north to south: Milky vent (marker N2), Marker 33 vent, Cloud Vent (markers N4 and N6), and Marker 113 vent (Figure S3, Supporting Information). The location for these markers has been fully described (Glazer and Rouxel 2009, Opatkiewicz et al. 2009, Deschamps et al. 2013, Fullerton et al. 2017).

In total, 33 MGCs were deployed and collected from the three locations, with two from Magic Mountain, 12 from Axial, and 19 from Kama'ehuakanaloa (Table 1). Each MGC was placed within the fluid flow at each venting location and all vent sites had either an abundance of iron- or sulfur-dominated mats. During the *in situ* incubations, temperatures at Axial ranged from 8.0 to 63.8°C, and at Magic Mountain temperatures ranged from 11.5 to 21°C. At Kama'ehuakanaloa, temperatures ranged from 12.5 to 77°C (Table 1).

Although these sites have been relatively well sampled, the timeframes for chemistry sampling do not align with the MGC incubation timeframes for all the samples. In general, though, Kama'ehuakanaloa is characterized by lower-temperature vents that have high concentrations of dissolved iron. Of the sampling locations at Kama'ehuakanaloa, Pohaku (Marker 57) has been routinely observed to have the highest abundance of Zetaproteobacteria. In 1996, an eruptive event at Kama'ehuakanaloa formed Pele's Pit, and high-temperature venting fluids were observed shortly after. Two sampling events shortly after the eruptive event recorded a decrease in thermal and fluid flux over 11 months (Wheat et al. 2000). However, the MGCs that were deployed in 1998 were incubated at the warmest of the observed temperatures at Kama'ehuakanaloa Seamount. Geochemistry sampling events in 2006, 2007, and 2008, showed Kama'ehuakanaloa had returned to a pre-eruption hydrothermal fluid composition (Glazer and Rouxel 2009). However, during the 2009 collections at Kama'ehuakanaloa, no fluid compositions were determined.

For Axial and Magic Mountain MGC incubation periods, pH and concentrations of hydrogen sulfide, total dissolved iron, and manganese were determined, and temperatures were measured. At Kama'ehuakanaloa, these measurements were only made for the 1998 and 2004 incubation periods (Table 2). The pH at Axial ranged from 4.86 to 6.89, which overlaps in the ranges for both Magic Mountain and Kama'ehuakanaloa. The concentrations of hydrogen sulfide were lowest at Kama'ehuakanaloa, and highest at Axial Seamount. Axial Seamount vent fluids were spatially and temporally variable over the period of MGC incubations (even though there was an eruptive event at Axial Seamount in 1998 a few months prior to our initial sampling). Axial vent fluids are generally sulfide-dominated with H_2S/Fe molar ratios from 2 to > 1000. In contrast, Kama'ehuakanaloa vent fluids are iron-dominated, with H_2S/Fe molar ratios from 0.01 to < 0.0001. Within the Kama'ehuakanaloa Seamount MGCs, the highest concentration of hydrogen sulfide was observed for the MGCs that were incubated shortly after the eruptive event. Concentrations of dissolved manganese were overall highest at Magic Mountain and two of the posteruption MGCs from Kama'ehuakanaloa. Dissolved iron was overall highest for the Kama'ehuakanaloa MGCs compared to the two highest concentrations measured in discharge where the Axial MGCs were deployed, even posteruption.

Table 2. Geochemical profiles associated with the MGCs.

MGC	pH	H_2S µmol/kg	dFe µmol/kg	Mn µmol/kg
AxMGC-01	5.55	762	76.50	2.50
AxMGC-03	5.73	446	10.30	3.50
AxMGC-05	5.04	1790	1.78	24.30
AxMGC-08	5.04	1790	1.78	24.30
AxMGC-10	5.04	1790	1.78	24.30
AxMGC-18	6.22	70	51.00	26.00
AxMGC-36	5.99	10.5	4.50	1.90
AxMGC-38	5.99	10.5	4.50	1.90
AxMGC-43	4.86	2320	1.28	34.20
AxMGC-44	5.80	123	1.97	19.70
AxMGC-47	5.95	123	15.50	8.09
AxMGC-66	6.89	5.03	6.77	4.60
ExMGC-03	5.48	315	11.80	104.30
ExMGC-04	5.29	559	20.10	89.30
LMGC-03	6.36	0.02	428.20	9.66
LMGC-04	5.92	0.00	59.60	1.15
LMGC-05	5.82	0.00	110.00	2.52
LMGC-07	5.82	0.00	110.00	2.52
LMGC-08	5.90	1.77	414.93	15.57
LMGC-09	6.32	0.01	75.10	3.47
LMGC-10	6.32	0.01	75.10	3.47
LMGC-L10	5.37	3.85	46.75	40.76
LMGC-L7	5.96	0.00	27.92	5.84
LMGC-L9A	5.37	3.85	46.75	40.76

Sequencing and community structure

A total of 11 451 454 paired-end sequences were used as the input into DADA2 for quality filtering and removal of chimeras which resulted in a total of 7 611 025 contigs remaining representing 9598 ASVs. There was no pattern of α-diversity detected as related to each Seamount, and increasing duration did not correspond to increased diversity (Figure S4, Supporting Information). For example, the observed ASVs were lowest in MGCs AxMGC-05, which was incubated for 16 days at Axial Seamount, and in LMGC-91, which was incubated for 5 days at Kama'ehuakanaloa Seamount. In these two MGCs, there were 102 and 107 ASVs, respectively (Table 1). The Chao1 and ACE species richness estimators show similar patterns to overall observed ASVs (Table S1, Supporting Information). Both alpha diversity estimators show LMGC-03, which was incubated Kama'ehuakanaloa for 4 days, to have the greatest count. The two MGCs from Magic Mountain, ExMGC-03 and ExMGC-04, were incubated for 4 days and were on the lower end with 544 and 140 observed ASVs. The MGCs with the lowest number of ASVs were not the most even as calculated by Simpson's index. MGC AxMGC-66 had the highest Simpson's value but also had 1158 ASVs by the Chao1 estimator. Conversely, MGC AxMGC-01 had the lowest Simpson's value, and the third-fewest ASVs by the Chao1 estimator.

Campylobacteria was the overwhelmingly dominant class identified in MGCs incubated at Axial and Magic Mountain whereas Zetaproteobacteria was the dominant class in the majority of the MGCs from Kama'ehuakanaloa, which hosted several other cooccurring classes as abundant community members. The class Campylobacteria was identified throughout all Axial and Magic Mountain MGCs but only found in 11 of the 19 MGCs from Kama'ehuakanaloa. Alphaproteobacteria and Gammaproteobacteria were abundant at Kama'ehuakanaloa and largely absent within the Axial and Magic Mountain MGCs (Fig. 2). Alphaproteobacteria and Bacteroidia, while found in many Kama'ehuakanaloa MGCs, made up less than 0.01% of the total communities from MGCs incubated at Axial Seamount or Magic Mountain. Interestingly, the three Kama'ehuakanaloa MGCs, LMGC-L9A, LMGC-L7, and LMGC-L10 incubated shortly after the eruptive event have a community composition that is distinct from any other MGCs, with a low abundance of Zetaproteobacteria and high abundance of Aquificae, Deinococci, and Campylobacteria (Fig. 2). In total, 606 ASVs were differentially abundant between Axial Seamount, Magic Mountain, and Kama'ehuakanaloa Seamount (Figure S5, Supporting Information). These ASVs ranged in abundance from over 50% to completely absent in a single MGC.

The bacterial communities were loosely grouped by marker location and seamount and did not group in the dendrogram by *in situ* temperature. In total, the bacterial communities of Axial and Magic Mountain were more similar to each other than to the communities of Kama'ehuakanaloa (Fig. 3). Three of the four Axial MGCs incubated at Marker N4 clustered together with AxMGC-47 separated from AxMGC-38 and AxMGC-36. The other MGC from Axial Marker N4, AxMGC-01, clustered with Axial MGCs from Marker 33 and one of the MGCs from Magic Mountain.

The clustering of MGCs incubated at Kama'ehuakanaloa showed a stronger influence of temporal variation than did those incubated at Axial and Magic Mountain: all Kama'ehuakanaloa MGCs collected in 2004 grouped together, inclusive of three incubation locations (Fig. 3). The four Marker 57 (Pohaku) MGCs formed a distinct cluster from the other MGCs at Kama'ehuakanaloa (e.g. LMGC-90, -92, -94, and -97). Interestingly, two of the Marker 38 MGCs, LMGC-05 and LMGC-07 from 2004, clustered separately from the other Marker 38 MGC, LMGC-96 from 2009. This same pattern was observed for MGCs incubated at Marker 36. The three MGCs from Hiolo North (Markers 36 and 39) clustered together for *in situ* incubations in 2009 but not in 2004.

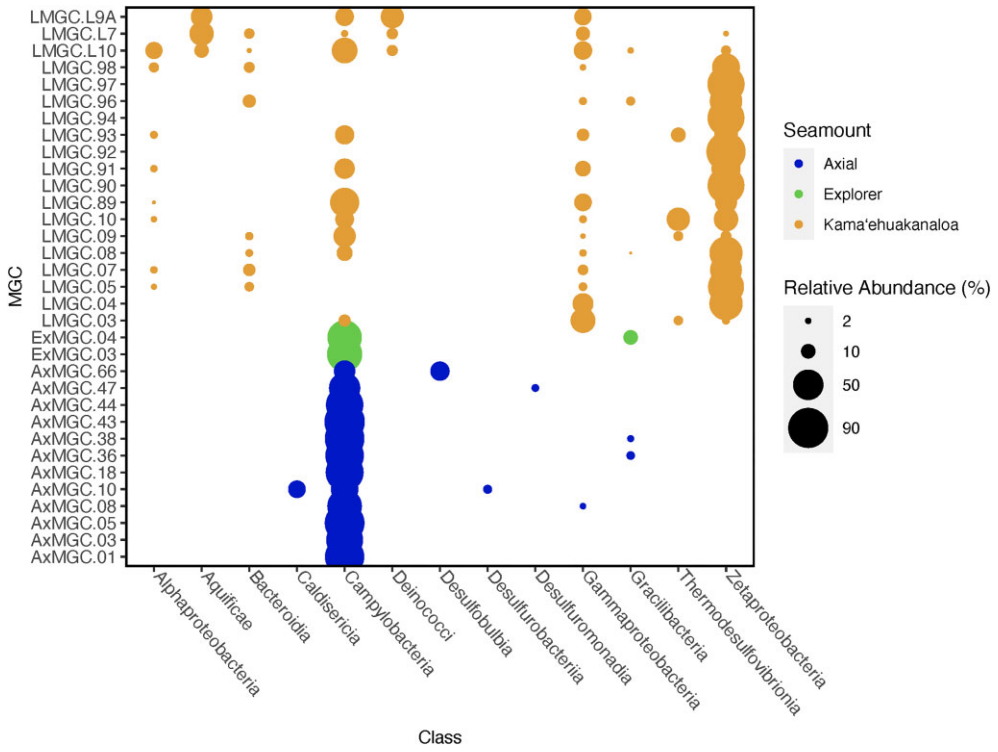

Figure 2. MGC community taxonomic distribution of top 1% abundant bacterial classes.

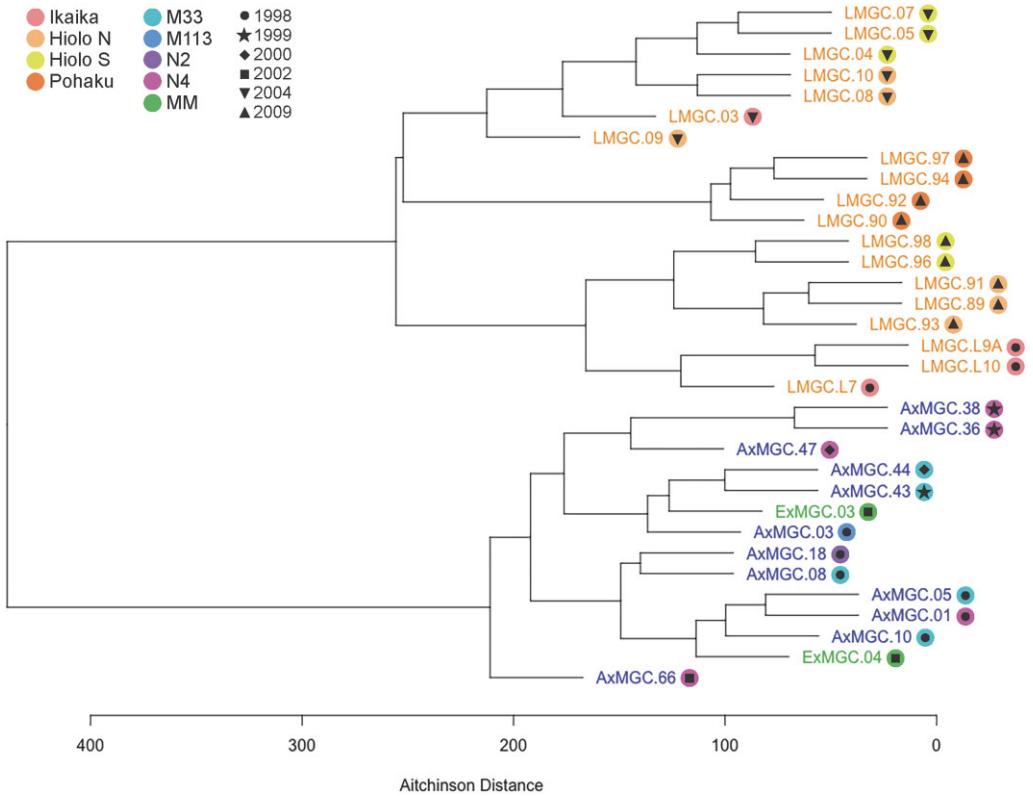

Figure 3. Hierarchical clustering of MGCs communities colored by *in situ* incubation location.

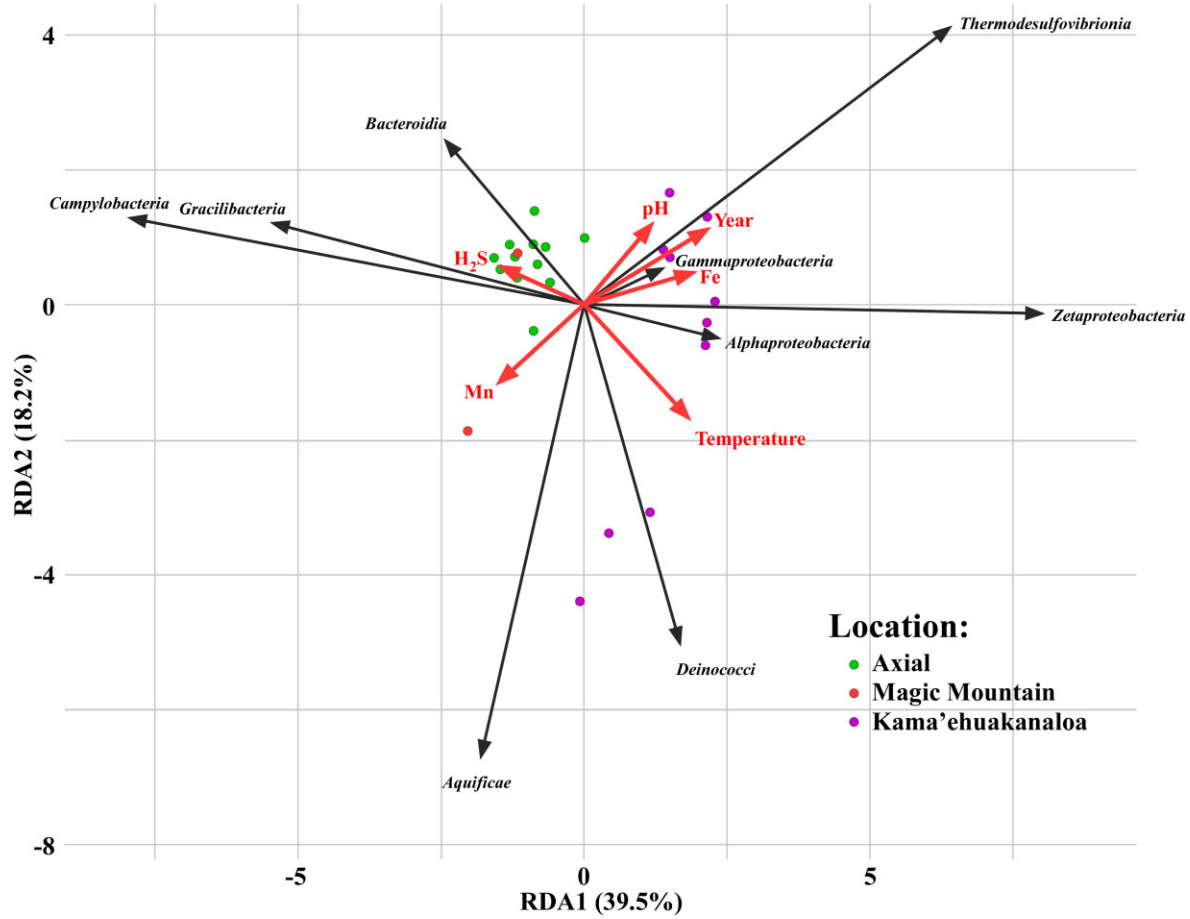

Figure 4. RDA of the top 10 most abundant bacterial classes within 24 MGCs at the three venting locations with selected environmental parameters that were shown to be significant by permanova.

The three samples from Kama'ehuakanaloa incubated shortly after the eruptive event in 1996 formed a unique cluster even though LMGC-L7 was incubated at a cooler temperature than LMGC-L10 and LMGC-L9A.

Duration and temperature were not able to be tested by permanova analysis for the complete set of MGCs because the assumption of homogenous within-group dispersions was not met. However, this criterion was met for seamount location and unsurprisingly is significant ($P = .001$). Further analysis was completed on Axial separate from Magic Mountain and Kama'ehuakanaloa. Temperature, duration, marker, and year were not significantly correlated with the MGC communities at Axial. However, when performing permanova on the Kama'ehuakanaloa MGCs to the exclusion of Axial and Magic Mountain, duration ($P = .011$) and year ($P = .044$) were significant factors in community composition. Magic Mountain microbial communities were represented by only two MGCs, therefore permanova analysis could not be performed.

Of the 33 MGCs, 24 had associated measurements of pH, hydrogen sulfide, dissolved iron, and manganese concentrations. To investigate geochemical parameters as drivers of the MGC community structure, permanova analysis was performed on that subset of 24 MGCs (Table S2, Supporting Information). Both duration and marker were unable to be tested since the within-group dispersions were significant. By permanova, pH ($P = .07$), and manganese ($P = .144$) were all nonsignificant factors in driving community composition. Whereas seamount ($P = .001$), year ($P = .001$), temperature ($P = .01$), hydrogen sulfide ($P = .034$), and dissolved iron ($P = .001$) were significant (Table S2, Supporting Information). Therefore, redundancy analysis was completed on the top 10 taxa by class and the chemistry parameters. From this, 57.7% of the variance was captured by RDA1 and RDA2 (Fig. 4). Dissolved iron and year were the most important factors in RDA1 and the abundance of Zetaproteobacteria correlated with the dissolved iron concentration. H_2S correlated with the Campylobacteria and inversely to the Zetaproteobacteria. By RDA analysis, Mn had inverse impacts on community structure than Fe and pH whereas H_2S was inversely correlated with temperature (Fig. 4). All locations with iron-dominated fluids from Kama'ehuakanaloa grouped with the Zetaproteobacteria, whereas the hot temperature MGCs from Kama'ehuakanaloa were ordinated more with temperature, along with Aquificae and Deinococci (Fig. 4).

Within the Campylobacteria, the genera *Sulfurovum* and *Sulfurimonas* were present in all MGCs from Axial and Magic Mountain (Fig. 5A). In total, nine of the 12 MGCs from Axial were dominated by *Sulfurovum* and the other three were dominated by *Thioreductor* and *Sulfurimonas*. On average, Campylobacteria accounted for 77.4% ± 16.6% of the ASVs across the MGCs from Axial and Magic Mountain. AxMGC-05 was 95.6% Campylobacteria, which was mostly *Sulfurovum* and *Sulfurimonas*. Only one sample from Axial or Magic Mountain had less than 50% Campylobacteria: AxMGC-66 with 36.6%, which was primarily *Sulfurovum*. That MGC also had the longest *in situ* incubation time and had a lower temperature with high concentration sulfide. Based on previous research at Axial, the dominance of these known sulfur-oxidizers

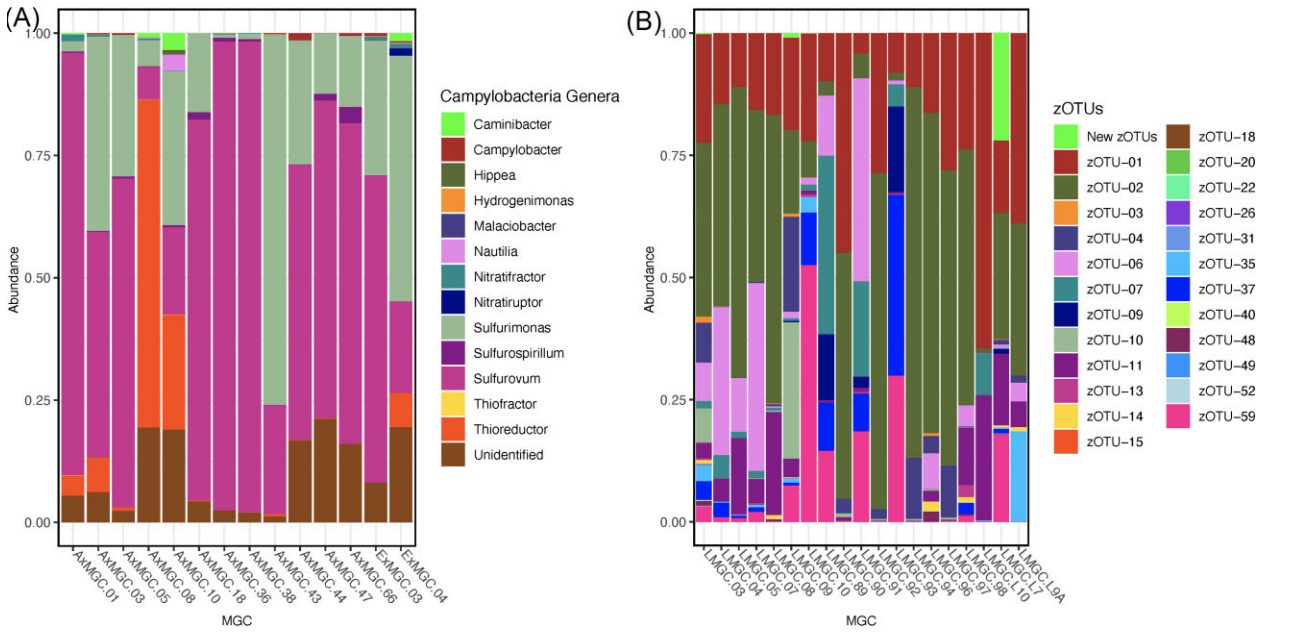

Figure 5. Stacked bar graphs showing (A) abundance of Campylobacteria genera at Axial and Magic Mountain Seamounts and (B) abundance of zOTUs at Kama'ehuakanaloa Seamount.

was expected. Zetaproteobacteria composed less than 0.05% of the total reads in the MGCs incubated Axial and Magic Mountain and were completely absent in four Axial MGCs (AxMGC-05, AxMGC-10, AxMGC-43, and AxMGC-44) and one Magic Mountain MGC (ExMGC-04). Those Zetaproteobacteria that were identified were predominately, the cosmopolitan taxa, zOTU-01 and zOTU-02.

In contrast, the MGCs from Kama'ehuakanaloa had a more variable Campylobacteria composition with three MGCs having abundant *Nitratiruptor* and six where *Sulfurimonas* was most dominant. Across all the MGCs from Kama'ehuakanaloa, Campylobacteria accounted for 13.8% of the total community and eight had less than 0.5% Campylobacteria. Zetaproteobacteria ranged in total population of the Kama'ehuakanaloa MGCs from 99% in LMGC-90 to only 2.8% in LMGC-L9A. zOTU-01 and zOTU-02 were present in all the Kama'ehuakanaloa MGCs and in 11 of these MGCs, zOTU-01 and zOTU-02 composed ≥ 50% of the total Zetaproteobacteria amplicons (Fig. 5B). One MGC, LMGC-L7, had a high abundance of "New zOTUs," which represent Zetaproteobacteria sequences that have not been classified into a previously identified zOTU (McAllister et al. 2018). Members of zOTUs 3, 9, 11, 14, 18, 23, 36, and 37 have cultured representatives, and only zOTUs 23 and 36 were not identified within the Kama'ehuakanaloa MGCs. Due to the high levels of reduced iron present at Kama'ehuakanaloa, it is unsurprising that Zetaproteobacteria were the most abundant class.

Fine-scale community analysis

A subset of the most dominant ASVs was further analyzed to better understand persistence among incubation timeframes. From the heatmap shown in Fig. 6, there is a clear distinction between the Kama'ehuakanaloa MGCs and the MGCs from Axial and Magic Mountain. Furthermore, the Kama'ehuakanaloa MGCs incubated after the eruptive event are also distinct from all other MGCs. Abundant ASVs in the Magic Mountain and Axial Seamount MGCs had very low abundances at Kama'ehuakanaloa and conversely, the abundant ASVs from Kama'ehuakanaloa had low abundances in the Magic Mountain and Axial MGCs. Only ASV-6, a *Sulfurimonas* spp., showed similar abundances across all MGC locations. ASV-56, also a *Sulfurimonas* spp., also showed high abundance at Kama'ehuakanaloa but was largely absent from Axial and Magic Mountain MGCs. zOTUs 1, 2, 6, 7, 11, 37, and 59 were represented in the most abundant ASVs (Table S3, Supporting Information). Cultured representatives of the Zetaproteobacteria were found in the MGC community, but none of them were identified in the topmost abundant ASVs.

An association network was constructed to visualize interactions among the most abundant ASVs. Two discrete clusters were formed within the network joined by strong mutual positive correlations and separated by weakly negative correlations between multiple ASVs within each cluster (Fig. 6B). One cluster was composed almost entirely of members of class Campylobacteria that were highly present in both Axial and Magic Mountain communities while having a low presence in Kama'ehuakanaloa MGC communities. The other cluster was largely composed of members of class Zetaproteobacteria with strong within-class positive correlations, but also included Campylobacteria, Aquificae, and Gammaproteobacteria, all of which were highly represented at Kama'ehuakanaloa. Regardless of cluster, the strongest correlations were positive, but several ASVs in the Kama'ehuakanaloa-dominated cluster correlated negatively to multiple ASVs in the Axial-Magic Mountain cluster. Interestingly, ASV-56, a *Sulfurimonas* spp. in the Kama'ehuakanaloa cluster (and found only in Kama'ehuakanaloa MGCs), exhibited the most abundant negative correlations, all to the Campylobacteria present in the Axial-Magic Mountain Campylobacteria cluster.

Of the Zetaproteobacteria present in the network analysis, zOTU-01 is represented by two distinct ASVs (ASV-5 and ASV-12) and zOTU-02 is represented by five different ASVs (ASV-1, ASV-4, ASV-22, ASV-27, and ASV-28). These ASVs showed a strong positive relationship to each other and to ASV-14, a *Roseobacter* within the class Alphaproteobacteria (Table S3, Supporting Information). The remainder of the zOTUs in this analysis are represented by a single ASV and were identified as zOTU-06, zOTU-07, zOTU-11, zOTU-37, and zOTU-59. Two cultured Zetaproteobacteria are present within

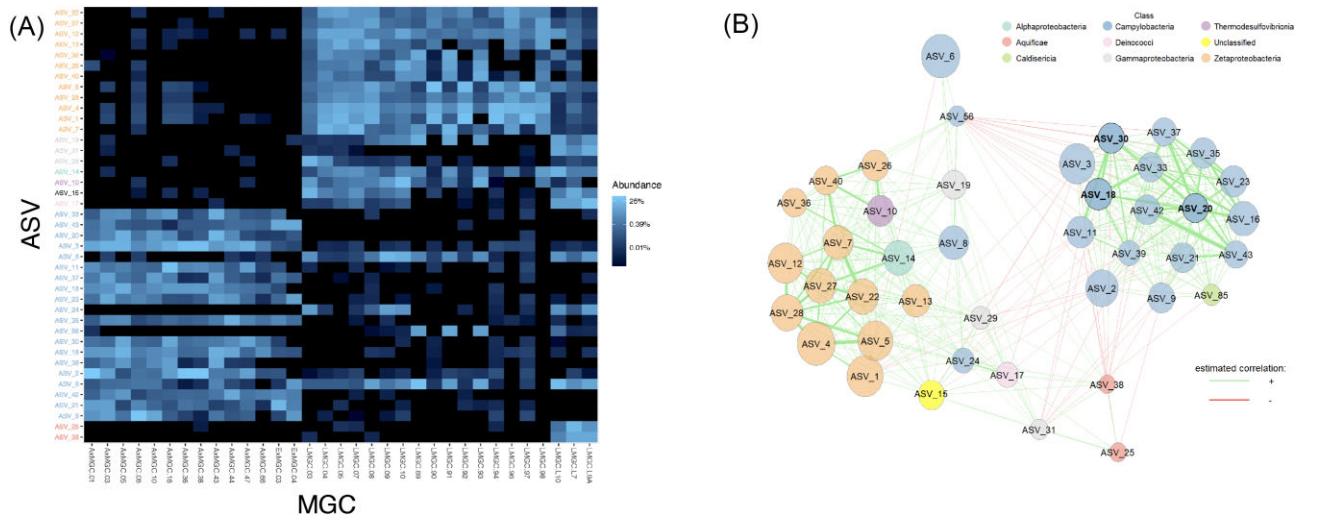

Figure 6. (A) Heatmap displaying abundance of the top 0.5% ASV within the MGCs from Axial, Magic Mountain, and Kama'ehuakanaloa Seamounts and (B) their interaction network. The color of nodes corresponds to bacterial class; edge colors correspond to positive (green) or negative (red) estimated correlation. Bold text indicates that the node acts as a hub.

this analysis, zOTU-11 and zOTU-37, which are represented by ASV-13 and ASV-40, respectively. Interestingly, the type strain of Zetaproteobacteria, zOTU-11, does not form strong relationships with any other ASVs. However, zOTU-37 forms a strong relationship with other Zetaproteobacteria and a *Thermodesulfovibrio*.

ASV-6, the only highly abundant Campylobacteria found in all three vent locations (Fig. 6A) clustered with Kama'ehuakanaloa Seamount but failed to show any strong correlations with other taxa (Fig. 6B). ASV-6 is identified as a *Sulfurimonas* spp. and is most similar to clones from Kama'ehuakanaloa Seamount and *S. autotrophica* OK10 by BLAST (data not shown). Three network hubs, representative of the most influential taxa in the network, were identified. All were Campylobacteria that were only found in the Axial-Magic Mountain cluster. Unsurprisingly, there were no positive correlations between the Zetaproteobacteria of the Kama'ehuakanaloa Seamount cluster and any of the Axial-Magic Mountain cluster ASVs, even though some Zetaproteobacteria were identified as minor community members of the MGCs from Axial and Magic Mountain.

Discussion

MGCs were placed within hydrothermal vent effluent to better understand the dynamics of microbial colonization at three Pacific Ocean hydrothermal vent sites. These incubations showed distinct microbial communities based on vent location, which relate to the predominant chemical composition of the discharging hydrothermal fluid. It is unclear if the nascent communities are developed from the dominant members of the existing microbial communities at these vents or if they are stochastically colonized. Alternatively, these nascent communities within the MGCs could represent ASVs that are adapted to growing on uncolonized surfaces. Shortly after the Kama'ehuakanaloa eruptive event, the colonizing community had a greater abundance of Campylobacteria and Aquificae compared to the incubations at cooler temperatures that had low sulfide concentrations, which were dominated by Zetaproteobacteria. Aquificae use hydrogen as their electron donor (Reysenbach 2001), however, hydrogen concentration was not analyzed with these collections. This shows that both the temperature and location of the vents have an influence on the microbial community composition. Additionally, the concentrations of iron and sulfide impact community composition resulting in low Campylobacteria abundance at Kama'ehuakanaloa Seamount when sulfide is also low in high-temperature incubations. Zetaproteobacterial isolates have narrow growth temperatures from 20 to 35°C whereas Campylobacterial isolates have a wider growth temperature from 20 to 70°C (Campbell et al. 2006, Nakagawa and Takai 2008, McAllister et al. 2019). When including the metadata collected alongside the MGCs, vent location, year, temperature, hydroten sulfide and dissolved iron were significant by permanova analysis. Given that several Campylobacteria ASVs were identified as keystone taxa, it was surprising that sulfide was determined to be a more minor driver of community structure. Conversely, it was unsurprising that dissolved iron was a driver of community structure since the zOTUs identified within the MGCs are hypothesized to be obligate iron-oxidizers and all tested sites had measurable amounts of dissolved iron. The function of dissolved iron as a driver of community structure was particularly intriguing at Kama'ehuakanaloa Seamount, where sampling year was also significant. Changes in community composition observed among sampling years could be due to the ephemeral nature of the discharging water (e.g. temperature, composition, and flow rate), or due to different *in situ* incubation durations.

Overall diversity and community differences across locations

Overall, the MGCs showed no pattern of diversity as related to duration of incubation or incubation temperatures. The year of MGC incubation was a significant factor for community composition in the MGCs, which is unsurprising due to the dynamic nature of these environments. However, even with this variation, the same ASVs are present within the MGCs per location, although their abundance varies among years of incubation and they have distinct ASVs as dominant community members. A previous study at the East Pacific Rise 13° N showed more phylotypes in short-term colonization experiments as compared to the longer-term incubations at the same site (Alain et al. 2004). In comparison to other deep-sea studies on microbial communities, we do not see patterns of succession as observed at whale and woodfall sites (Goffredi and Orphan 2010, Kalenitchenko et al. 2016). This could be

due to the relatively short incubation times or the constant influx of reduced substrates in hydrothermal fluids.

Other deep-sea colonization experiments performed on rock chips have noted evidence of a changing community over time and microbially driven chemical weathering (Orcutt et al. 2011a, Gulmann et al. 2015). Previous studies have shown a higher diversity in mature iron-dominated microbial mats than those that are sulfur-dominated in the Mariana Arc and back-arc (Hager et al. 2017). However, this pattern of higher diversity in high dissolved iron sites was not observed in the MGC microbial communities. Microbial mat surfaces, which are hypothesized to contain the active fraction in mature mats, show a wider range in richness as measured by Chao1 (Chan et al. 2016b, Duchinski et al. 2019). This indicates that the MGCs are lower in taxonomic diversity than that of established microbial mats. With the decreased microbial diversity of nascent mat communities, as represented by the MGCs, there is likely to be less functional diversity than that found in established communities as well (Wagg et al. 2021).

Gammaproteobacteria that were identified from Kama'ehuakanaloa MGCs have also been found in established microbial mats from Kama'ehuakanaloa and the Mariana Arc and back-arc, though the lack of these taxa within the Axial and Magic Mountain MGCs is in contrast to previous studies of vent fluids at Axial Seamount (Huber et al. 2003, Opatkiewicz et al. 2009, Rassa et al. 2009, Hager et al. 2017, Duchinski et al. 2019). The nascent community composition from Axial Seamount and Magic Mountain was similar to active hydrothermal chimneys that are dominated by *Sulfurimonas* and *Sulfurovum* as found within vent fluids at Manus Basin (Meier et al. 2017, 2019) and from Brother's Volcano (Zhou et al. 2022). Hydrothermal minerals from the Juan de Fuca Ridge have been shown to support the iron-oxidizing autotrophic growth of both Alphaproteobacteria and Gammaproteobacteria isolates (Edwards et al. 2003). These classes also track with dissolved iron concentrations in our study, though less so than the Zetaproteobacteria.

Zetaproteobacteria diversity

Both Campylobacteria and Zetaproteobacteria are chemolithoautotrophs and can support a diversity of microorganisms and macrofauna. Genomic and proteomic analysis of Zetaproteobacteria show autotrophy is supported by the Calvin–Benson–Bassham cycle (Singer et al. 2011, Barco et al. 2015). Conversely, autotrophic Campylobacteria and Aquificae primarily use the reverse TCA cycle for carbon fixation (Hügler and Sievert 2011). Zetaproteobacteria have been shown to produce twisted iron-oxyhydroxide biominerals, which contribute to the mat architecture (Chan et al. 2016a). Within the MGCs, zOTU-01 zOTU-02 were the most dominant, which is expected since they have been found in high abundance within established mats at iron-dominated hydrothermal vent communities (McAllister et al. 2019). The metabolism of these dominant zOTUs has been inferred from single cell-genomes and metagenome-assembled genomes (Field et al. 2015, Fullerton et al. 2017), and both show the capacity for living in aerobic conditions and fixing carbon. The organisms represented by these zOTUs also contain a fused cytochrome-porin that is responsible for the oxidation of dissolved Fe^{2+} (Keffer et al. 2021), which is conserved across the genus *Mariprofundus* (Zhong et al. 2022). It is unclear if the Zetaproteobacteria are growing via hydrogen oxidation since only zOTU-09 is known with this metabolism (Mori et al. 2017) and was present as minor community members within six of the 19 MGCs incubated at Kama'ehuakanaloa.

Campylobacteria composition

Diverse genera within the phylum Campylobacterota have been shown to inhabit hydrothermal vent plumes, sulfides, and the vent subsurface (Sylvan et al. 2012b, Dick et al. 2013, Meyer et al. 2013b). Overall, Campylobacteria were nearly universal within this study, but genera varied between locations. Even in the high-temperature Kama'ehuakanaloa Seamount MGCs, the Campylobacteria ASVs were distinct from those found within the Axial Seamount or Magic Mountain MGCs, as was the case for ASV-24 (*Nitratiruptor* spp.), which was found only within the Kama'ehuakanaloa Seamount MGCs. It was not surprising that *Sulfurimonas* and *Sulfurovum* were present as dominant representatives of Campylobacteria at Kama'ehuakanaloa and were also present in Axial and Magic Mountain MGCs; due to their diverse metabolisms, they can live in various conditions by using different energy sources (Nakagawa et al. 2005, Campbell et al. 2006). These groups of bacteria are not only able to use sulfur but also have a pathway for NO_3^- reduction (Han and Perner 2015, Pérez-Rodríguez et al. 2017). Of the identified ASVs, ASV-6, a *Sulfuromonas* spp., was found in varying abundances throughout all MGCs, suggesting it is a hydrothermal vent cosmopolitan Campylobacteria. Where there was a dominance of Campylobacteria, the Zetaproteobacteria were minor community members. The high abundance of Campylobacteria and Aquificae at Kama'ehuakanaloa after the eruption is representative of how the geochemistry of the active vent shifted the microbial community. This is in contrast to other studies from 1998 to 1999 where the diversity of Campylobacteria decreased after a previous eruption at Axial Seamount (Huber et al. 2003).

Community interactions

Overall, our results indicate that the concentration of dissolved iron from the vent fluids favors the growth of Zetaproteobacteria as the dominant primary producer. Based on the permanova analysis, the influence of pH and Mn were not significant in these communities. This is consistent with the RDA analysis and the community interaction, which indicate that the bacterial community is significantly affected by the abundance of Zetaproteobacteria and with their role as ecosystem engineers (Chan et al. 2011, Hager et al. 2017, Beam et al. 2018).

Although the two classes, Zetaproteobacteria and Campylobacteria, were foundational members of these nascent communities, only the Campylobacteria formed hubs in network analysis, which indicate keystone taxa (Peschel et al. 2021). Two ASVs from class Aquificae formed positive associations with the Zetaproteobacteria in the Kama'ehuakanaloa cluster, despite their lack of co-occurrence in time, while also forming negative associations with the Campylobacteria from the Axial-Magic Mountain cluster despite the earlier noted tendency for Aquificae and Campylobacteria to cooccur. These seemingly contradictory associations further support the significance of geographic location as a driver of community structure. Within the Zetaproteobacteria, the most influential community members were identified as belonging to zOTU-06 (ASV_7) and zOTU-02 (ASV_27, ASV_22, and ASV_28) (Table S3, Supporting Information). However, they did not meet the cutoff requirement for hub classification and so are not considered as keystone taxa, which is in contrast to other iron-rich marine environments (Beam et al. 2018). Additionally, the Gammaproteobacteria were found throughout the nascent communities at Kama'ehuakanaloa and within only one Axial MGC. Only a few Gammaproteobacteria ASVs formed positive relationships with foundational members of those communities, and only with the Zetaproteobacteria.

Conclusion

This study builds on the knowledge of community diversity and composition of lithotrophic bacteria, providing new data from three Pacific Ocean hydrothermal vent locations. Our results indicate that diverse microbial communities form quickly within hydrothermal vent effluent and are dominated by chemolithoautotrophs. SSU rRNA amplicon sequencing from 33 MGCs showed relatively low alpha diversity overall. There was also no difference in diversity across incubation periods and each site showed distinct microbial community composition. This supports the influence of biogeography as well as the impact of geochemistry on microbial diversity across these vent locations. Although Shannon and Simpson's diversity indices did not show correlation with age of MGC, future comparisons should be performed between the mature and nascent microbial mat to further understand the drivers of diversity.

Also of note was the reduction in the abundance of iron-oxidizing Zetaproteobacteria after the Kama'ehuakanaloa eruption, which instead displayed a higher abundance of Campylobacteria. Observing such shifts is important to understanding how the biogeochemistry of the surrounding area affects autotrophic microbial communities. Additionally, further research should focus on determining if the community members present within the MGCs are also present in the vent fluids or if they are members of the adjacent microbial mats.

Future studies should include longer incubation periods to further determine whether patterns of succession are different for these habitats as opposed to whale and woodfalls. In addition, a simultaneous study of vent fluids, established microbial mats, and MGC composition should be conducted to understand whether the community composition is the same across these substrates under the same incubation conditions.

Author contributions

Heather Fullerton (Conceptualization, Formal analysis, Investigation, Methodology, Project administration, Visualization, Writing – original draft, Writing – review & editing), Lindsey Smith (Formal analysis, Visualization, Writing – original draft, Writing – review & editing), Alejandra Enriquez (Writing – original draft, Writing – review & editing), David Butterfield (Data curation, Methodology, Writing – review & editing), C. Geoffrey Wheat (Data curation, Writing – review & editing), and Craig L. Moyer (Conceptualization, Data curation, Funding acquisition, Writing – original draft, Writing – review & editing)

Acknowledgments

We wholeheartedly thank the operation teams for ROPOS, Pisces V and Jason II, and the captains and crew of the R/Vs Kaimikai-o-Kanaloa, Melville, Kilo Moana, and Thomas G. Thompson for their assistance with sample collection during oceanographic research cruises in 1998, 2000, 2002, 2004, and 2009.

Supplementary data

Supplementary data is available at *FEMSEC Journal* online.

Conflict of interest: None declared.

Funding

This project was funded in part by then National Science Foundation awards MCB-0348734 (to C.L.M.), by the Fout Foundation for the Enhancement of Student Research Experiences (to C.L.M.), and the College of Charleston Department of Biology Research and Development fund (to H.F.). Additional funding from NOAA/PMEL, NOAA Ocean Exploration, and the Cooperative Institute for Climate, Ocean, & Ecosystem Studies (CICOES) under NOAA Cooperative Agreement NA20OAR4320271, Contribution number 2023-1323, PMEL Contribution number 5567.

Data availability

All sequence data are available through the NCBI Sequence Read Archive study number SUB11788075 (BioProject: PRJNA858068). Hydrothermal fluid compositions are provided in Table 2.

References

Akerman NH, Butterfield DA, Huber JA. Phylogenetic diversity and functional gene patterns of sulfur-oxidizing subseafloor epsilonproteobacteria in diffuse hydrothermal vent fluids. *Front Microbiol* 2013;**4**:1–14.

Alain K, Zbinden M, Le Bris N *et al.* Early steps in microbial colonization processes at deep-sea hydrothermal vents. *Environ Microbiol* 2004;**6**:227–41.

Anderson RE, Reveillaud J, Reddington E *et al.* Genomic variation in microbial populations inhabiting the marine subseafloor at deep-sea hydrothermal vents. *Nat Commun* 2017;**8**. https://doi.org/10.1038/s41467-017-01228-6.

Barco RA, Emerson D, Sylvan JB *et al.* New insight into microbial iron oxidation as revealed by the proteomic profile of an obligate iron-oxidizing chemolithoautotroph. *Appl Environ Microbiol* 2015;**81**:5927–37.

Beam JP, Scott JJ, McAllister SM *et al.* Biological rejuvenation of iron oxides in bioturbated marine sediments. *ISME J* 2018;**12**:1389–94. https://doi.org/10.1038/s41396-017-0032-6.

Butterfield DA, Jonasson IR, Massoth GJ *et al.* Seafloor eruptions and evolution of hydrothermal fluid chemistry [and Discussion]. *Philos Trans Math, Phys Eng Sci* 1997;**355**:369–86.

Butterfield DA, Roe KK, Lilley MD *et al.* Mixing, reaction and microbial activity in the sub-seafloor revealed by temporal and spatial variation in diffuse flow vents at axial volcano. In: Wilcock WSD, DeLong EF, Kelley DS al. et (eds), *Geophysical Monograph Series*. Vol. **144**, Washington: American Geophysical Union, 2004, 269–89.

Callahan BJ, McMurdie PJ, Holmes SP. Exact sequence variants should replace operational taxonomic units in marker-gene data analysis. *ISME J* 2017;**11**:2639–43.

Callahan BJ, McMurdie PJP, Rosen MJM *et al.* DADA2: high-resolution sample inference from Illumina amplicon data. *Nat Methods* 2016;**13**:581–3.

Campbell BJ, Engel AS, Porter ML *et al.* The versatile ε-proteobacteria: key players in sulphidic habitats. *Nat Rev Microbiol* 2006;**4**:458–68.

Cerqueira T, Barroso C, Froufe H *et al.* Metagenomic signatures of microbial communities in deep-sea hydrothermal sediments of Azores vent fields. *Microb Ecol* 2018;**76**:387–403. https://doi.org/10.1007/s00248-018-1144-x.

Chan CS, Emerson D, Luther GW. The role of microaerophilic Fe-oxidizing microorganisms in producing banded iron formations. *Geobiology* 2016a;**14**. https://doi.org/10.3837/tiis.0000.00.000.

Chan CS, Mcallister SM, Leavitt AH *et al.* The architecture of iron microbial mats reflects the adaptation of chemolithotrophic iron oxidation in freshwater and marine environments. *Front Microbiol* 2016b;**7**:1–18.

Chan CS, Fakra SC, Emerson D *et al.* Lithotrophic iron-oxidizing bacteria produce organic stalks to control mineral growth: implications for biosignature formation. *ISME J* 2011;**5**:717–27.

Chiu BK, Kato S, McAllister SM *et al.* Novel pelagic iron-oxidizing zetaproteobacteria from the Chesapeake Bay oxic-anoxic transition zone. *Front Microbiol* 2017;**8**:1–16.

Danovaro R, Canals M, Tangherlini M *et al.* A submarine volcanic eruption leads to a novel microbial habitat. *Nat Ecol Evol* 2017;**1**:0144.

Deschamps A, Tivey MA, Chadwick WW *et al.* Waning magmatic activity along the Southern Explorer Ridge revealed through fault restoration of rift topography. *Geochem Geophys Geosyst* 2013;**14**:1609–25.

Dick GJ, Anantharaman K, Baker BJ *et al.* The microbiology of deep-sea hydrothermal vent plumes: ecological and biogeographic linkages to seafloor and water column habitats. *Front Microbiol* 2013;**4**:1–16.

Dick GJ. The microbiomes of deep-sea hydrothermal vents: distributed globally, shaped locally. *Nat Rev Microbiol* 2019;**17**:271–83.

Duchinski K, Moyer CL, Hager KW *et al.* Fine-scale biogeography and the inference of ecological interactions among neutrophilic iron-oxidizing zetaproteobacteria as determined by a rule-based microbial network. *Front Microbiol* 2019;**10**:1–11.

Edwards KJ, Rogers DR, Wirsen CO *et al.* Isolation and characterization of novel psychrophilic, neutrophilic, Fe-oxidizing, chemolithoautotrophic α- and γ-Proteobacteria from the deep sea. *Appl Environ Microbiol* 2003;**69**:2906–13.

Emerson D, Rentz JA, Lilburn TG *et al.* A novel lineage of proteobacteria involved in formation of marine Fe-oxidizing microbial mat communities. *PLoS ONE* 2007;**2**:e667.

Engebretson J. The terminal-restriction fragment length polymorphism assay and its use in determining bacterial community succession at hydrothermal vents. Master's Thesis, WWU Biology Dept., 2002;**82**.

Erb I, Notredame C. How should we measure proportionality on relative gene expression data?. *Theory Biosci* 2016;**135**:21–36.

Erb I, Quinn T, Lovell D *et al.* Differential proportionality—a normalization-free approach to differential gene expression. In: *Proceedings of CoDaWork 2017, the 7th Compositional Data Analysis Workshop, Abbadia San Salvatore, Italy*. Girona: CoDa-Association, 2017, 1–16.

Field EK, Sczyrba A, Lyman AE *et al.* Genomic insights into the uncultivated marine *Zetaproteobacteria* at Loihi Seamount. *ISME J* 2015;**9**:857–70.

Fortunato CS, Larson B, Butterfield DA *et al.* Spatially distinct, temporally stable microbial populations mediate biogeochemical cycling at and below the seafloor in hydrothermal vent fluids: microbial genomics at Axial Seamount. *Environ Microbiol* 2018;**20**:769–84.

Fullerton H, Hager KW, McAllister SM *et al.* Hidden diversity revealed by genome-resolved metagenomics of iron-oxidizing microbial mats from Lō'ihi Seamount, Hawai'i. *ISME J* 2017;**11**:1–15.

Glazer BT, Rouxel OJ. Redox speciation and distribution within diverse iron-dominated microbial habitats at Loihi Seamount. *Geomicrobiol J* 2009;**26**:606–22.

Goffredi SK, Orphan VJ. Bacterial community shifts in taxa and diversity in response to localized organic loading in the deep sea. *Environ Microbiol* 2010;**12**:344–63.

Gulmann LK, Beaulieu SE, Shank TM *et al.* Bacterial diversity and successional patterns during biofilm formation on freshly exposed basalt surfaces at diffuse-flow deep-sea vents. *Front Microbiol* 2015;**6**:1–16.

Hager KW, Fullerton H, Butterfield DA *et al.* Community structure of lithotrophically-driven hydrothermal microbial mats from the Mariana Arc and Back-Arc. *Front Microbiol* 2017;**8**. https://doi.org/10.3389/fmicb.2017.01578.

Han Y, Perner M. The globally widespread genus Sulfurimonas: versatile energy metabolisms and adaptations to redox clines. *Front Microbiol* 2015;**6**:1–17.

He S, Barco RA, Emerson D *et al.* Comparative genomic analysis of neutrophilic iron (II) oxidizer genomes for candidate genes in extracellular electron transfer. *Front Microbiol* 2017;**8**:1–17.

Huber JA, Butterfield DA, Baross JA. Bacterial diversity in a subseafloor habitat following a deep-sea volcanic eruption. *FEMS Microbiol Ecol* 2003;**43**:393–409.

Huber JA, Cantin HV, Huse SM *et al.* Isolated communities of *Epsilonproteobacteria* in hydrothermal vent fluids of the Mariana Arc seamounts. *FEMS Microbiol Ecol* 2010;**73**:538–49.

Hügler M, Sievert SM. Beyond the Calvin cycle: autotrophic carbon fixation in the ocean. *Ann Rev Mar Sci* 2011;**3**:261–89.

Inagaki F, Takai K, Kobayashi H *et al.* *Sulfurimonas autrotrophica* gen. nov., sp. nov., a novel sulfur-oxidizing E-proteobacterium isolated from hydrothermal sediments in the Mid-Okinawa Trough. *Int J Syst Evol Microbiol* 2003;**53**:1801–5.

Jannasch HW, Mottl MJ. Geomicrobiology of deep-sea hydrothermal vents. *Science* 1985;**229**:717–25.

Jannasch HW. Microbial processes at deep sea hydrothermal vents. In: *Hydrothermal Processes At Seafloor Spreading Centers: NATO Conference Series*. Vol. **12**, Boston: Springer, 1983, 677–709.

Jesser KJ, Fullerton H, Hager KW *et al.* Quantitative PCR analysis of functional genes in iron-rich microbial mats at an active hydrothermal vent system (Lō'ihi Seamount, Hawai'i). *Appl Environ Microbiol* 2015;**81**:2976–84.

Kalenitchenko De, Dupraz M, Le Bris N *et al.* Ecological succession leads to chemosynthesis in mats colonizing wood in sea water. *ISME J* 2016;**10**:2246–58.

Karl DM, Wirsen CO, Jannasch HW. Deep-sea primary production at the Galapagos hydrothermal vents. *Science* 1980;**207**:1345–7.

Karl DM. Ecology of free-living, hydrothermal vent microbial communities. In: Karl DM (ed.), *Microbiology of Deep-Sea Hydrothermal Vents*. Boca Raton: CRC Press, 1995, 35–124.

Keffer JL, McAllister SM, Garber AI *et al.* Iron oxidation by a fused cytochrome-porin common to diverse Iron-oxidizing bacteria. *mBio* 2021;**12**. https://doi.org/10.1128/mbio.01074-21.

Klindworth A, Pruesse E, Schweer T *et al.* Evaluation of general 16S ribosomal RNA gene PCR primers for classical and next-generation sequencing-based diversity studies. *Nucleic Acids Res* 2013;**41**:1–11.

Lahti L, Shetty S. microbiome R package. GitHub, 2017.

Lee MD, Walworth NG, Sylvan JB *et al.* Microbial communities on seafloor basalts at Dorado Outcrop reflect level of alteration and highlight global lithic clades. *Front Microbiol* 2015;**6**:1–20.

Love MI, Huber W, Anders S. Moderated estimation of fold change and dispersion for RNA-seq data with DESeq2. *Genome Biol* 2014;**15**:550.

Lovell D, Pawlowsky-Glahn V, Egozcue JJ *et al.* Proportionality: a valid alternative to correlation for relative data. *PLoS Comput Biol* 2015;**11**:1–12.

Makita H, Tanaka E, Mitsunobu S *et al.* *Mariprofundus micogutta* sp. nov., a novel iron-oxidizing zetaproteobacterium isolated from a deep-sea hydrothermal field at the Bayonnaise knoll of the Izu-Ogasawara Arc, and a description of *Mariprofundales ord*. nov. and *Zetaproteobacteria classis* nov. *Arch Microbiol* 2017;**199**:335–46.

Martin M. Cutadapt removes adapter sequences from high-throughput sequencing reads. *EMBnet J* 2011;**17**:10–2.

McAllister SM, Davis RE, McBeth JM *et al.* Biodiversity and emerging biogeography of the neutrophilic iron-oxidizing *Zetaproteobacteria*. *Appl Environ Microbiol* 2011;**77**:5445–57.

McAllister SM, Moore RM, Chan CS. ZetaHunter, a reproducible taxonomic classification tool for tracking the ecology of the *Zetaproteobacteria* and other poorly resolved taxa. *Microbiol Resour Announc* 2018;**7**:1–3.

McAllister SM, Moore RM, Gartman A *et al.* The Fe(II)-oxidizing *Zetaproteobacteria* : historical, ecological and genomic perspectives. *FEMS Microbiol Ecol* 2019;**95**:1–18.

McMurdie PJ, Holmes S. phyloseq: an R package for reproducible interactive analysis and graphics of microbiome census data. *PLoS ONE* 2013;**8**:e61217.

Meier DV, Pjevac P, Bach W *et al.* Microbial metal-sulfide oxidation in inactive hydrothermal vent chimneys suggested by metagenomic and metaproteomic analyses. *Environ Microbiol* 2019;**21**:682–701.

Meier DV, Pjevac P, Bach W *et al.* Niche partitioning of diverse sulfur-oxidizing bacteria at hydrothermal vents. *ISME J* 2017;**11**:1545–58.

Meyer JL, Akerman NH, Proskurowski G *et al.* Microbiological characterization of post-eruption "snowblower" vents at Axial Seamount, Juan de Fuca Ridge. *Front Microbiol* 2013a;**4**:1–13.

Meyer S, Wegener G, Lloyd KG *et al.* Microbial habitat connectivity across spatial scales and hydrothermal temperature gradients at Guaymas Basin. *Front Microbiol* 2013b;**4**:1–11.

Mino S, Nakagawa S, Makita H *et al.* Endemicity of the cosmopolitan mesophilic chemolithoautotroph Sulfurimonas at deep-sea hydrothermal vents. *ISME J* 2017;**11**:909–19.

Mori JF, Scott JJ, Hager KW *et al.* Physiological and ecological implications of an iron- or hydrogen-oxidizing member of the *Zetaproteobacteria*, *Ghiorsea bivora*, gen. nov., sp. nov. *ISME J* 2017 ;**11**:1–13.

Moulana A, Anderson RE, Fortunato CS *et al.* Selection is a significant driver of gene gain and loss in the pangenome of the bacterial genus Sulfurovum in geographically distinct deep-sea hydrothermal vents. *mSystems* 2020;**5**:1–18.

Murdock SA, Tunnicliffe V, Boschen-Rose RE *et al.* Emergent "core communities" of microbes, meiofauna and macrofauna at hydrothermal vents. *ISME Commun* 2021;**1**:27.

Nakagawa S, Takai K, Inagaki F *et al.* Distribution, phylogenetic diversity and physiological characteristics of epsilon-proteobacteria in a deep-sea hydrothermal field. *Environ Microbiol* 2005;**7**:1619–32.

Nakagawa S, Takai K. Deep-sea vent chemoautotrophs: diversity, biochemistry and ecological significance. *FEMS Microbiol Ecol* 2008;**65**:1–14.

Opatkiewicz AD, Butterfield DA, Baross JA. Individual hydrothermal vents at Axial Seamount harbor distinct subseafloor microbial communities. *FEMS Microbiol Ecol* 2009;**70**:413–24.

Orcutt BN, Bach W, Becker K *et al.* Colonization of subsurface microbial observatories deployed in young ocean crust. *ISME J* 2011a;**5**:692–703.

Orcutt BN, Sylvan JB, Knab NJ *et al.* Microbial ecology of the dark ocean above, at, and below the seafloor. *Microbiol Mol Biol Rev* 2011b;**75**:361–422.

Parks DH, Chuvochina M, Waite DW *et al.* A standardized bacterial taxonomy based on genome phylogeny substantially revises the tree of life. *Nat Biotechnol* 2018;**36**:996.

Pérez-Rodríguez I, Sievert SM, Fogel ML *et al.* Biogeochemical N signatures from rate-yield trade-offs during in vitro chemosynthetic NO_3^- reduction by deep-sea vent ε-proteobacteria and aquificae growing at different temperatures. *Geochim Cosmochim Acta* 2017;**211**:214–27.

Peschel S, Müller CL, Von Mutius E *et al.* NetCoMi: network construction and comparison for microbiome data in R. *Brief Bioinf* 2021;**22**:1–18.

Price MT, Fullerton H, Moyer CL. Biogeography and evolution of thermococcus isolates from hydrothermal vent systems of the Pacific. *Front Microbiol* 2015;**6**:1–12.

Quinn TP, Erb I, Gloor G *et al.* A field guide for the compositional analysis of any-omics data. *GigaScience* 2019;**8**:1–14.

Quinn TP, Erb I, Richardson MF *et al.* Understanding sequencing data as compositions: an outlook and review. *Bioinformatics* 2018;**34**:2870–8.

Quinn TP, Richardson MF, Lovell D *et al.* Propr: an R-package for identifying proportionally abundant features using compositional data analysis. *Sci Rep* 2017;**7**:1–9.

Rassa AC, McAllister SM, Safran Sa *et al.* Zeta-Proteobacteria dominate the colonization and formation of microbial mats in low-temperature hydrothermal vents at Loihi Seamount, Hawaii. *Geomicrobiol J* 2009;**26**:623–38.

Reysenbach A-L., Phylum BI. Aquificae *phy. nov*. In: Boone DR, Castenholz RW (eds), *Bergey's Manual of Systematic Bacteriology*. 2nd edn. Berlin, Heidelberg: Springer, 2001, 359–67.

Scott JJ, Breier JA, Luther GW *et al.* Microbial iron mats at the Mid-Atlantic Ridge and evidence that *Zetaproteobacteria* may be restricted to iron-oxidizing marine systems. *PLoS ONE* 2015;**10**:e0119284.

Singer E, Emerson D, Webb EA *et al.* *Mariprofundus ferrooxydans* PV-1 the first genome of a marine Fe(II) oxidizing zetaproteobacterium. *PLoS ONE* 2011;**6**:e25386.

Sylvan JB, Pyenson BC, Rouxel O *et al.* Time-series analysis of two hydrothermal plumes at 9°50′N East Pacific Rise reveals distinct, heterogeneous bacterial populations. *Geobiology* 2012a;**10**:178–92.

Sylvan JB, Toner BM, Edwards KJ. Life and death of deep-sea vents: bacterial diversity and ecosystem succession on inactive hydrothermal sulfides. *mBio* 2012b;**3**:1–10.

Vetriani C, Voordeckers JW, Crespo-Medina M *et al.* Deep-sea hydrothermal vent *Epsilonproteobacteria* encode a conserved and widespread nitrate reduction pathway (Nap). *ISME J* 2014;**8**:1510–21. https://doi.org/10.1038/ismej.2013.246.

Von Damm KL, Edmond JM, Grant B *et al.* Chemistry of submarine hydrothermal solutions at 21 °N, East Pacific Rise. *Geochim Cosmochim Acta* 1985;**49**:2197–220.

Wagg C, Hautier Y, Pellkofer S *et al.* Diversity and asynchrony in soil microbial communities stabilizes ecosystem functioning. *eLife* 2021;**10**:e62813.

Waite DW, Vanwonterghem I, Rinke C *et al.* Comparative genomic analysis of the class *Epsilonproteobacteria* and proposed reclassification to epsilonbacteraeota (phyl. nov.). *Front Microbiol* 2017;**8**. https://doi.org/10.3389/fmicb.2017.00682.

Waite DW, Vanwonterghem I, Rinke C *et al.* Erratum: Addendum: Comparative Genomic Analysis of the Class *Epsilonproteobacteria* and Proposed Reclassification to Epsilonbacteraeota (phyl. nov.). *Front Microbiol* 2018;**9**:772.

Wheat CG, Fisher AT, McManus J *et al.* Cool seafloor hydrothermal springs reveal global geochemical fluxes. *Earth Planet Sci Lett* 2017;**476**:179–88.

Wheat CG, Jannasch HW, Plant JN *et al.* Continuous sampling of hydrothermal fluids from Loihi Seamount after the 1996 event. *J Geophys Res* 2000;**105**:19353–67.

Yoon G, Gaynanova I, Müller CL. Microbial networks in SPRING—semi-parametric rank-based correlation and partial correlation estimation for quantitative microbiome data. *Front Genet* 2019;**10**. https://doi.org/10.3389/fgene.2019.00516.

Zhong YW, Zhou P, Cheng H *et al.* Genome sequence of five *Zetaproteobacteria* metagenome-assembled genomes recovered from hydrothermal vent Longqi, Southwest Indian Ridge. *Mar Geonomics* 2022;**63**:100936.

Zhou Z, St. John E, Anantharaman K *et al.* Global patterns of diversity and metabolism of microbial communities in deep-sea hydrothermal vent deposits. *Microbiome* 2022;**10**: 241.

Received 23 May 2023; **revised** 20 October 2023; **accepted** 9 January 2024